

Effect of the Pressure on the Crystallization Behavior of Polyamide 66

J. C. WON,¹ R. FULCHIRON,² A. DOUILLARD,² B. CHABERT,² J. VARLET,³ D. CHOMIER⁴

¹ Korea Research Institute of Chemical Technology, Advanced Materials Division, P.O. Box 107, Yusong, Taejeon 305-606, South Korea

² Laboratoire des Matériaux Polymères et des Biomatériaux, UMR CNRS #5627, Université Lyon 1, Bat ISTIL, 43, Bd 11 Novembre 1918, 69622 Villeurbanne Cedex, France

³ CRL—Rhodia-Recherches, 85 av. des Frères Perret, BP 62, 69192 Saint Fons Cedex, France

⁴ Rhodia-Engineering-Plastics, Avenue Ramboz, BP 64, 69192 Saint Fons Cedex, France

Received 16 November 1999; accepted 5 June 2000

ABSTRACT: The crystallization behavior of polyamide 66 under high pressure up to 2500 bar was investigated by the use of dilatometric and calorimetric techniques in nonisothermal and isothermal conditions. The solid–solid Brill transition is detected from the evolution of the specific volume in the PVT diagram. The variation of supercooling was examined under different pressures and temperatures. In nonisothermal conditions, when the same cooling rate is applied, the crystallization supercooling is not changed for different pressures. In isothermal conditions, for a given temperature, a pressure increase extends the crystallization supercooling. By the analysis of melting peaks of samples crystallized in different conditions of pressure and temperature, we can conclude that the increasing of the crystallization supercooling leads to a decrease of the lamellae thickness. Finally, the evolution of the thermodynamic equilibrium melting temperature according to pressure was examined. © 2001 John Wiley & Sons, Inc. *J Appl Polym Sci* 80: 1021–1029, 2001

Key words: polyamide 66; crystallization; supercooling; Brill transition; pressure; equilibrium melting temperature

INTRODUCTION

Polyamide 66 (PA66) is one of the most famous engineering thermoplastics because of its excellent physical and mechanical properties.^{1,2} Its applications are found in most industries and markets: transportation, packaging, textile, electronic and electric components, etc. During the process, the polymer is molten and then solidified, in spe-

cific conditions of temperature and pressure, particularly for injection molding. Besides, especially in the case of a semicrystalline polymer, some shrinkage appears during the process. Therefore, the knowledge of the crystallization of a semicrystalline polymer is of a great importance for the manufacture of plastic parts because physical properties are dependent on the crystalline morphology. Moreover, the crystallization of PA66 has been investigated by a number of experimental studies. However, there has not been yet a systematic study of the pressure effects on its morphology.

For this reason, we studied the effect of the pressure on the crystallization of PA66. The pres-

Correspondence to: R. Fulchiron.

Contract grant sponsor: Rhodia Nyltech Co.

Journal of Applied Polymer Science, Vol. 80, 1021–1029 (2001)
© 2001 John Wiley & Sons, Inc.

sure influence was investigated in nonisothermal and isothermal conditions, by use of high-pressure dilatometry [pressure–volume–temperature (PVT)], differential scanning calorimetry (DSC), and polarized light optical microscopy. Then, the crystallization temperature and the morphology were analyzed considering the evolution of the equilibrium melting temperature (T_m^0) of PA66 according to the pressure.

Moreover, the stable crystalline structure of PA66 at room temperature is denoted as the α -phase (triclinic) and constituted of sheets built owing to hydrogen bonds. The intersheet stacking is controlled by van der Waals interactions. But, at higher temperature, the structure is turned into the γ -phase, which is a pseudo-hexagonal structure³ where the hydrogen bonds are distributed in the three directions. The Brill transition⁴ concerns the formation of this pseudo-hexagonal structure and it is found in many polyamides.^{5–10} In this study, the pressure effect on the Brill transition was also investigated.

EXPERIMENTAL

In this work, the studied PA66 was supplied by the Rhodia Nyltech Co. (Sant-Fons, France) with two formulations: a virgin grade and a commercial grade nucleated for injection-productivity enhancement. The molecular weight of the polymer was $M_w = 33000 \text{ g mol}^{-1}$, determined by viscosimetry in formic acid (90 vol %) at 30°C. The crystallization study was carried out in nonisothermal and isothermal conditions between 200 and 2500 bar.

The crystallization was investigated by measuring the change of specific volume under high pressure using an apparatus PVT-100 from SWO Polymertechnik. Dilatometric measurements determined the relationship among the specific volume, the temperature, and the pressure. This apparatus can work between room temperature and 420°C with a precision of $\pm 0.3^\circ\text{C}$ and between 200 and 2500 bar with a precision of $\pm 5\%$. The sample of 0.6–0.9 g is introduced into the cylinder (diameter: 7.8 mm) and the pressure is applied by the upper mobile piston. VESPEL (polyimide) sealings are used to prevent leakage of the polymer during the experiment. The specific volume is determined from the measurement of the sample length. The main inconvenience of the piston technique is that, in the solid state, due to a Poisson coefficient lower than 0.5, the pressure is not hydrostatic¹¹ on the sample, leading to

an error on the specific volume measurements. Nevertheless, by comparison with the results of He and Zoller,^{12,13} who used a fluid-type PVT technique for the crystallization of PA66 in nonisothermal conditions, we obtained similar results for the evolution of the specific volume with the pressure during crystallization with a discrepancy less than 2%.

Before each crystallization experiment, the sample was dried for 16 h at 110°C in a vacuum oven. The sample was precompressed up to 2000 bar, at 310°C, during 1 min, to remove the air. Then, the desired pressure was applied. The sample was maintained at high temperature during 10 min to eliminate the thermal history. In nonisothermal conditions, the behavior of PA66 was studied at several cooling rates between 2.5 and 15°C min⁻¹, under different pressures between 200 and 2500 bar. In isothermal conditions, the specific volume was recorded at different temperatures under 400 and 800 bar. According to the crystallization temperature, the experiment duration was between 30 min and 6 h. After each isothermal crystallization, the obtained semicrystalline polymer was submitted to a rapid cooling to 30°C.

Some samples, crystallized under high pressure, were analyzed by DSC on the heating process at 10°C/min using a DSC7 from Perkin-Elmer. The morphology was observed by polarized light optical microscopy. The preparation of the sample was carried out by a microtome (thickness $\approx 10 \mu\text{m}$).

RESULTS AND DISCUSSION

Nonisothermal Crystallization

The evolution of the specific volume in nonisothermal conditions exhibits a sharp decrease between the molten state and the solid state as shown in Figure 1. The crystallization temperature (T_c) increases according to a pressure increase. This variation can be largely explained by the evolution of the equilibrium melting temperature (T_m^0), which is the melting temperature for a hypothetical infinite-size crystal. When the pressure increases, the entropy of the liquid decreases, which leads to an increase of the free enthalpy of the liquid. The curves of the liquid and the solid free enthalpy cross at a higher temperature, as seen in Figure 2. Hence, the equilibrium melting temperature is increased. Moreover, since the crystallization is driven mainly by

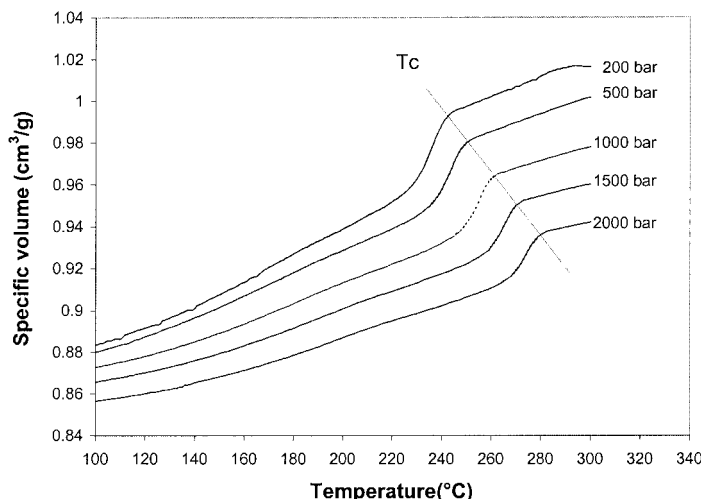


Figure 1 Evolution of the specific volume of the virgin PA66 at various pressures in nonisothermal conditions (cooling rate: 5°C min⁻¹).

the supercooling ($\Delta T = T_m^\circ - T$), an increase of T_m° leads to an increase of the crystallization temperature.

From the specific volume measurement in nonisothermal conditions, the relative crystallinity versus the temperature can be obtained:

$$X(T) = \frac{V_a - V_T}{V_a - V_s} \quad (1)$$

where V_a is the liquid-state specific volume extrapolated at temperature T ; V_s , the solid-state specific volume extrapolated at temperature T ; and V_T , the specific volume measured at temperature T .

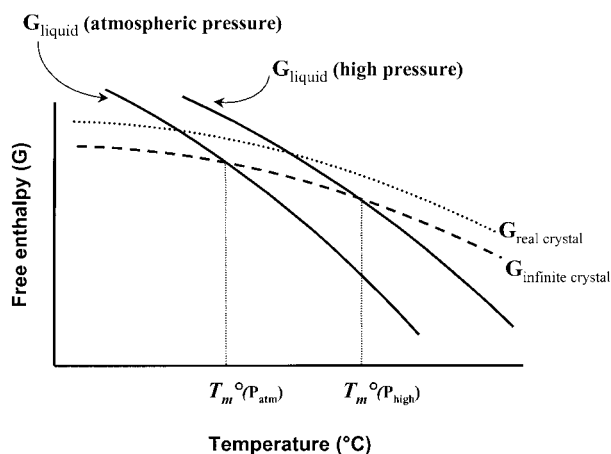


Figure 2 Scheme of the pressure effect on the equilibrium melting temperature from a free-enthalpy viewpoint.

It should be pointed out that for PA66 the baseline extrapolated from the solid-state specific volume is sometimes ambiguous because it does not clearly appear as a linear part. This is due mainly to the Brill transition.⁴ Figure 3 shows the evolution of the half-crystallization temperature ($T_{1/2}$), that is, the temperature corresponding to 50% of the relative crystallinity. As already mentioned, the crystallization temperature increases when the pressure increases for the same cooling rate.

Moreover, the samples crystallized under pressure were analyzed in the heating mode by DSC (10°C/min). As shown in Figure 4, the melting traces of virgin PA66 samples crystallized at 10°C/min under different pressures are superimposed. So, it can be concluded that the morphology is independent of the pressure for the same cooling rate. Indeed, the melting peaks arise for the same temperature, indicating that the lamellae thickness is identical and the peak area is constant, bearing out that the crystallinity is the same. This conclusion is confirmed by polarized light microscopy which exhibits an identical size of spherulites for different crystallization pressures but at the same cooling rate (see Fig. 5). Therefore, considering that the crystalline morphology is governed mainly by the crystallization supercooling, it can be concluded that, for a given cooling rate, the crystallization occurs for the same supercooling whatever the crystallization pressure. In other words, the effect of the pressure is counterbalanced by the increase of the crystallization temperature, leading to an unchanged crystallization supercooling.

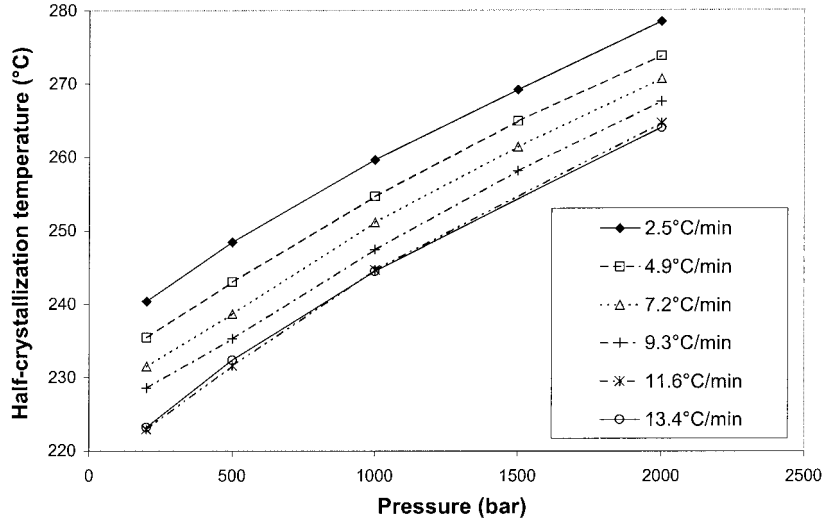


Figure 3 Evolution of the half-crystallization temperature ($T_{1/2}$) versus the pressure at various cooling rates.

Furthermore, considering that the crystallization supercooling is pressure-independent, the equilibrium melting temperature and the crystallization temperature must depend on the pressure in the same way. Besides, the half-crystallization temperature $T_{1/2}$ evolution with the pressure can be described by a second-order polynomial:

$$T_{1/2}(p) = a + bp + cp^2 \quad (2)$$

Then, the equilibrium melting temperature is expressed by

$$T_m^\circ(p) = T_{m,1\text{bar}}^\circ + bp + cp^2 \quad (3)$$

where the coefficients b and c are the same as in eq. (2) and $T_{m,1\text{bar}}^\circ$ is the equilibrium melting temperature at atmospheric pressure (280°C for PA66).

It should be mentioned that this kind of evolution for the melting temperature of polymers is well known.^{14,15} Obviously, since the equilibrium melting temperature is a thermodynamic parameter, it depends only on the nature of the polymer and the pressure. So, in eq. (2), a is the unique

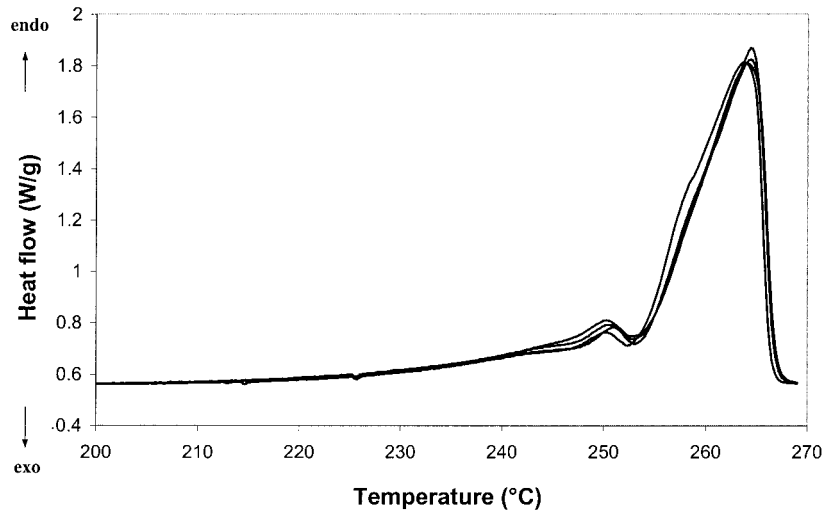


Figure 4 Melting peaks of virgin PA66 crystallized under 400, 1200, 2000, and 2500 bar with the same cooling rate of 10°C/min.

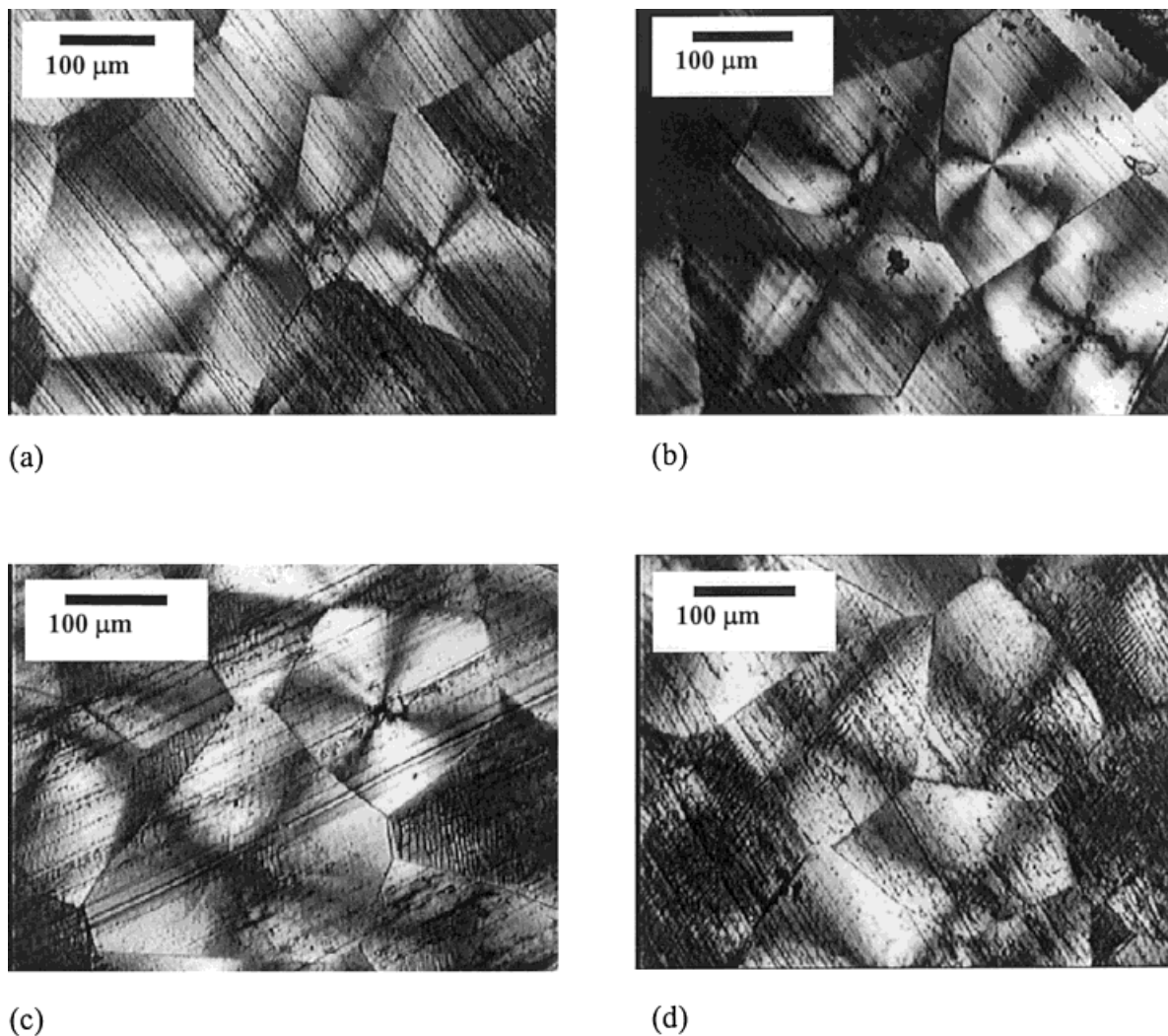


Figure 5 Polarized light micrographs of virgin PA66 crystallized with the same cooling rate of 10°/min, under different pressures: (a) 400 bar; (b) 1200 bar; (c) 2000 bar; (d) 2500 bar.

parameter which depends on the cooling rate or the formulation since b and c appear in eq. (3).

The coefficients b and c , calculated with the values of $T_{1/2}$ obtained for a cooling rate of 7.5°C min⁻¹, are 2.82×10^{-2} K bar⁻¹ and -2.84×10^{-6} K bar⁻², respectively. To verify these results, the relative crystallinity curves obtained with two cooling rates (2.5 and 10°C min⁻¹) for two formulations (virgin and nucleated) are plotted in Figure 6 versus the supercooling expressed by

$$\Delta T = T_m^\circ(p) - T = T_{m,1\text{bar}}^\circ + bp + cp^2 - T \quad (4)$$

As shown in Figure 6, for the same cooling rate and the same formulation, all the relative crystallinity curves are superimposed whatever the

pressure. Moreover, using the same values for parameters b and c , this superposition is achieved for different cooling rates and for the virgin or the nucleated PA66. This issue clearly indicates that these parameters depend only on the nature of the polymer and that they reflect the pressure dependence of the equilibrium melting temperature. Moreover, in Figure 7, the supercooling corresponding to the half-crystallization versus the cooling rate is plotted for the virgin and nucleated polyamides and for different pressures, leading to the same conclusion since the results are independent of the pressure.

Furthermore, from a thermodynamic point of view, parameter b can also be evaluated using the Clapeyron equation¹⁶:

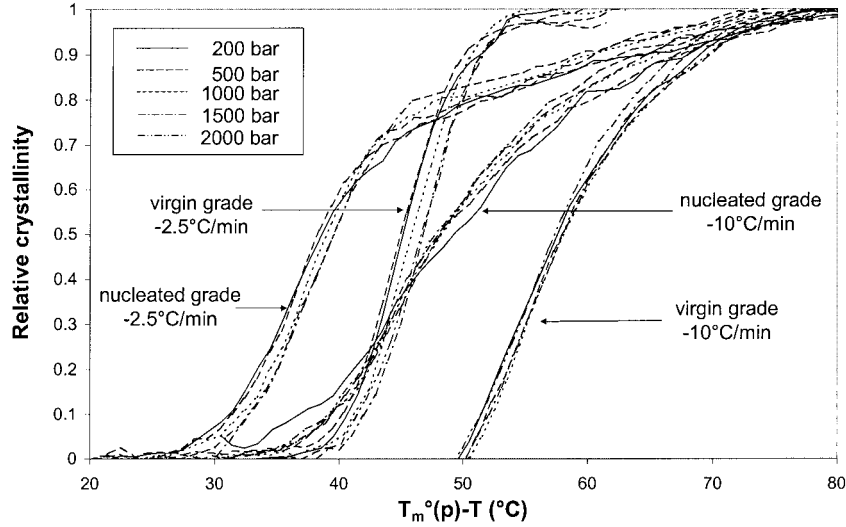


Figure 6 Evolution of the relative crystallinity versus the supercooling ($b = 2.82 \times 10^{-2} \text{ K bar}^{-1}$, $c = -2.84 \times 10^{-6} \text{ K bar}^{-2}$).

$$b = \left. \frac{dT_m^\circ}{dp} \right|_{p_{atm}} = \frac{T_m^\circ \Delta V}{\Delta H_f} \quad (5) \quad V_{sp}(P, T) = V_{sp}(0, T) \left\{ 1 - C \ln \left[1 + \frac{P}{B(T)} \right] \right\}$$

$$V_{sp}(0, T) = V_0 \exp(\alpha_0 T) \quad (6)$$

$$B(T) = B_0 \exp(-B_1 T)$$

where $\Delta V = V_a - V_c$ is the specific volume difference between the liquid and the pure crystalline phases and ΔH_f is the heat of fusion per unit mass.

As for applying eq. (5), it is necessary to assess the specific volume difference at T_m° . The specific volume of the amorphous phase at this temperature can be evaluated from the Tait equation¹⁷:

where $C = 0.0894$ is a universal constant, and $V_{sp}(0, T)$, the specific volume at atmospheric pressure.

Using the specific volume measurements in the liquid state, the Tait equation parameters were

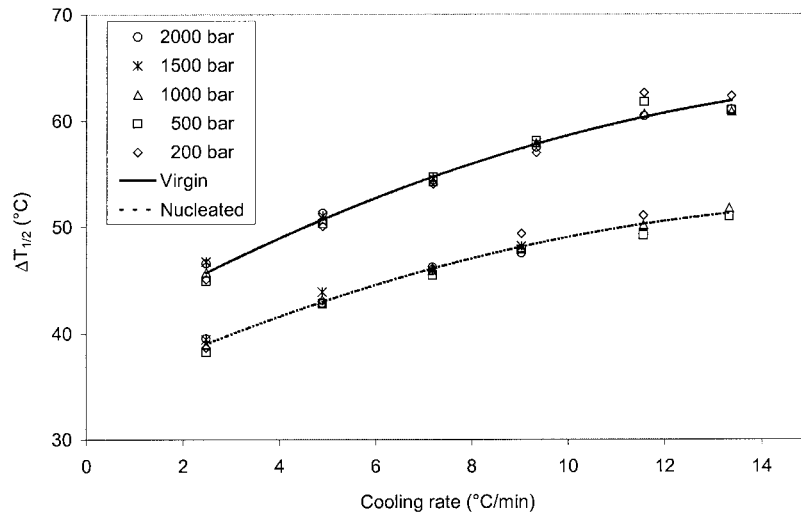


Figure 7 Evolution of the half-crystallization supercooling according to cooling rate at different pressures.

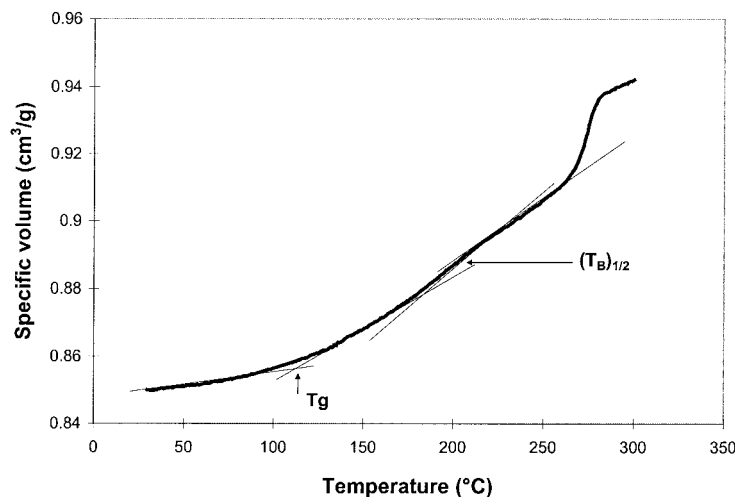


Figure 8 Highlight of the second transition for PA66 (cooling rate: $5^{\circ}\text{C min}^{-1}$ at 2000 bar).

adjusted, leading to $V_0 = 0.889 \text{ cm}^{-3} \text{ g}^{-1}$, $\alpha_0 = 4.97 \times 10^{-4} \text{ }^{\circ}\text{C}^{-1}$, $B_0 = 3793 \text{ bar}$, and $B_1 = 3.67 \times 10^{-3} \text{ }^{\circ}\text{C}^{-1}$. Then, the specific volume of the amorphous phase at atmospheric pressure and 280°C can be evaluated: $V_a = 1.0214 \text{ cm}^3 \text{ g}^{-1}$.

The specific volume of the crystalline phase at 280°C and atmospheric pressure was estimated using the results of Starkweather et al.¹⁸ who measured the evolution of the crystal density of PA66 as a function of the temperature. Their works shown that the specific volume of the crystal increases to 200°C but remains constant between 200 and 250°C and equals $0.920 \text{ cm}^3 \text{ g}^{-1}$. For a temperature higher than 250°C , the measurement cannot be achieved because of the polymer melting. Considering that the crystal specific volume at 280°C is $0.920 \text{ cm}^3 \text{ g}^{-1}$ and using a heat of fusion equal to 196 J/g , eq. (5) leads to $dT_m/dp = 2.89 \times 10^{-2} \text{ K bar}^{-1}$, which is very close to the obtained value of b .

Brill Transition

As already mentioned, in the solid state, the evolution of the specific volume of PA66 is not clearly defined as a linear part. Indeed, a second transition appears at a lower temperature than the main crystallization temperature, between 150 and 240°C , as shown in Figure 8. It seems that this can be attributed to the Brill transition,⁴ that is, a solid–solid transition. This transition is generally detected by X-ray diffraction, but not easily by differential scanning calorimetry (DSC) because the enthalpy difference between the two

structures is very small. Nevertheless, it can be observed by dilatometry since the density difference between the two crystalline forms is sufficiently important.

We denoted this transition by the temperature corresponding to the half-transition $[(T_B)_{1/2}]$ (see Fig. 8). The evolution of the $(T_B)_{1/2}$ appears quasilinear versus the pressure, as shown in Figure 9. The extrapolation to the atmospheric pressure leads to the value of 152°C . This value does not agree with the reported one by Starkweather and Jones¹⁹ who obtained $199 \pm 4^{\circ}\text{C}$, but their measurement was carried out by a heating procedure at atmospheric pressure, while our experiments were carried out in a cooling mode. Ramesh et al.⁸ observed the transition at 160°C by a cooling procedure and Hirschinger et al.⁹ reported the transition between 139 and 169°C , which is in agreement with our result.

Isothermal Crystallization

Different isothermal crystallizations were carried out under 400 and 800 bar in the isothermal mode. As an example, Figure 10 shows the evolution of the specific volume for different temperatures under 800 bar .

Using eq. (3), the equilibrium melting temperatures under 400 and 800 bar are 290.8 and 300.7°C , respectively (difference of about 10°C). To analyze the morphology, isothermal crystallizations at 260°C under 400 and 800 bar of pressure and at 270°C under 800 bar of pressure were carried out. The samples were then analyzed by DSC in heating process at $10^{\circ}\text{C min}^{-1}$. The cor-

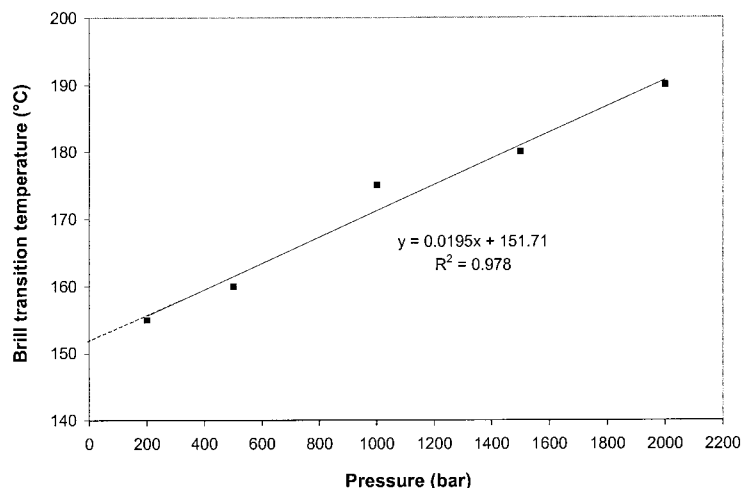


Figure 9 Evolution of the Brill half-transition temperature $[(T_B)_{1/2}]$ for PA66 (cooling rate: 5°C min^{-1}).

responding thermograms are shown in Figure 11. The melting peak of the sample crystallized under 800 bar at 260°C appears at a lower temperature than for the sample crystallized under 400 bar at 260°C . So, for the same crystallization temperature, the lamellae thickness is higher when the pressure is lower, because the crystallization supercooling is lower. When the crystallization temperature is changed from 260 to 270°C , under the same pressure of 800 bar, the melting peak is moved toward the higher temperature, leading to a thermogram similar to the melting curve of the sample crystallized at 260°C and 400 bar, meaning that both samples exhibit the same lamellae thickness. These experiments confirm that a vari-

ation of the crystallization pressure from 400 to 800 bar and a simultaneous variation of the crystallization temperature from 260 to 270°C leads to a similar supercooling.

CONCLUSIONS

In nonisothermal conditions when experiments are realized at a same cooling rate, the crystallization supercooling is not changed by the variation of the pressure because the increase of pressure leads to an increase of the thermodynamic equilibrium melting temperature, but this effect is counterbalanced by the increase of the crystal-

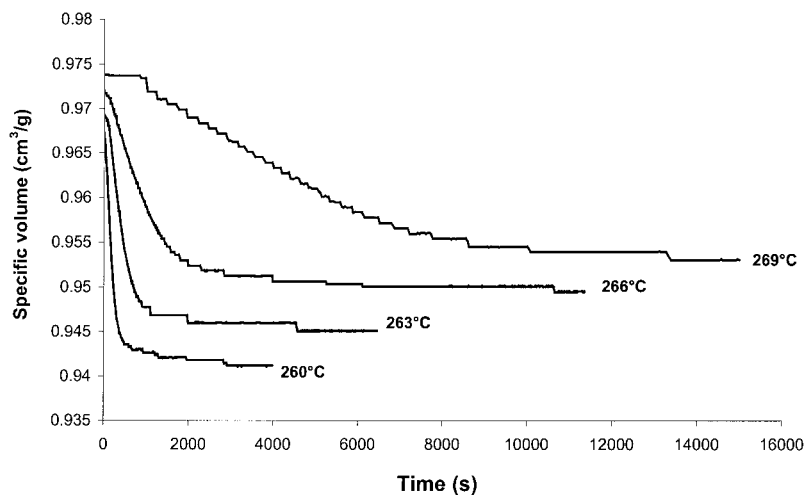


Figure 10 Evolution of the specific volume of PA66 for different crystallization temperatures under 800 bar.

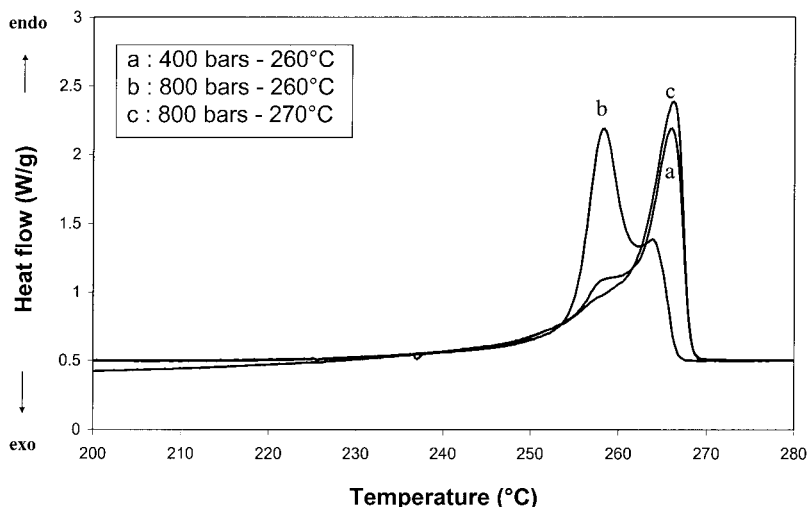


Figure 11 Melting curves of samples crystallized at different pressures in the isothermal condition.

lization temperature. So, the obtained morphology is independent of the pressure. However, when the cooling rate increases, the crystallization supercooling increases, modifying the final morphology.

The evolution of the thermodynamic equilibrium melting temperature according to the pressure can be represented by a second-order curve. The value of dT_m^c/dp at atmospheric pressure is $2.82 \times 10^{-2} \text{ K bar}^{-1}$.

In isothermal conditions, for a given crystallization temperature, the increase of the pressure raises the crystallization supercooling, leading to thinner crystalline lamellae. Moreover, the Brill transition of PA66 is detected using dilatometry in nonisothermal conditions. This transition appears between 150 and 190°C according to the pressure between atmospheric pressure and 2000 bar.

The authors would like to thank the Rhodia Nyltech Co. for its financial support and material supply.

REFERENCES

1. Dominghaus, H. *Plastics for Engineers: Materials, Properties, Applications*; Hanser: Munich, 1988; Chapter 13.
2. Welgos, R. J. In *Encyclopedia of Polymer Science and Engineering*, 2nd ed.; Mark, H. F.; Bikales, N. M.; Overberger, C. G.; Menges, G., Eds.; Wiley: New York, 1988; Vol. 11, pp 445–476.
3. Bunn, C. W.; Garner, E. V. *Proc R Soc Lond A* 1947, 189, 39.
4. Brill, R. *Macromol Chem* 1956, 18/19, 294.
5. Itoh, T. *Jpn J Appl Phys* 1976, 15, 2295.
6. Murthy, N. S.; Curran, S. A.; Aharoni, S. M.; Minor, H. *Macromolecules* 1991, 24, 3215.
7. Jones, N. A.; Atkins, E. D. T.; Hill, M. J.; Cooper, S. J.; Franco, L. *Macromolecules* 1996, 29, 6011.
8. Ramesh, C.; Keller, A.; Eltink, S. J. E. A. *Polymer* 1994, 35, 2483.
9. Hirschinger, J.; Miura, H.; Gardner, K. H.; English, A. D. *Macromolecules* 1990, 23, 2153.
10. Cooper, S. J.; Atkins, E. D. T.; Hill, M. J. *Macromolecules* 1998, 31, 8947.
11. Lei, M.; Reid, C. G.; Zoller, P. *Polymer* 1988, 29, 1784.
12. He, J.; Zoller, P. *ANTEC 92* 1992, 1144.
13. He, J. Thesis, University of Colorado, Colorado, 1992; 166 pp.
14. Davidson, T.; Wunderlich, B. *J Polym Sci A-2* 1969, 7, 377.
15. Kishore, K.; Vasanthakumari, R. *High Temp High Press* 1984, 16, 241–268.
16. Ihm, D. W.; Cuculo, J. A. *J Polym Sci Polym Chem* 1982, 20, 1847.
17. Wang, Y. Z.; Chia, W. J.; Hsieh, K. H.; Tseng, H. C. *J Appl Polym Sci* 1992, 44, 1731.
18. Starkweather, H. W., Jr.; Zoller, P.; Jones, G. A. *J Polym Sci Polym Phys* 1984, 22, 1615.
19. Starkweather, H. W., Jr.; Jones, G. A. *J Polym Sci Polym Phys* 1981, 19, 467.